The Journal of Neuroscience, July 1991, 11(7): 2075–2086

Immunohistochemical Localization of an Inositol 1,4,5-Trisphosphate Receptor, P_{400}, in Neural Tissue: Studies in Developing and Adult Mouse Brain

Setsuko Nakanishi,[1,2] Nobuaki Maeda,[1,a] and Katsuhiko Mikoshiba[1]

[1]Division of Regulation of Macromolecular Function, Institute for Protein Research, Osaka University, 3-2, Yamadaoka, Suita 565, Japan and [2]Research Laboratory, Susumu Co., Ltd., 14, Umamawashicho, Kamitoba, Minamiku, Kyoto 601, Japan

The immunohistochemical localization of P_{400}/inositol 1,4,5-trisphosphate ($InsP_3$) receptor protein was studied in developing and adult mouse brain by using monoclonal antibodies. The developmental expression pattern of $P_{400}/InsP_3$ receptor protein differed among different classes of neurons. It was first detected in the somata of immature Purkinje cells at embryonic day 17, in the ventrolateral region of the posterior vermis in the cerebellum. Axonal immunoreactivity within the cerebellar nuclei was first present at postnatal day 3. Neurons in the retrosplenial cortex, the anterior olfactory nucleus, and the CA1 region of the hippocampus expressed immunoreactivity earlier than other regions of the brain. In the adult brain, not only the Purkinje cell but also many other types of cells in many areas of the brain expressed $P_{400}/InsP_3$ receptor, though to a lesser extent. These included the neurons in the striatum, globus pallidus, nucleus accumbens septi, anterior olfactory nucleus, olfactory tubercle, precommissural hippocampus, hippocampus, substantia nigra, cerebral cortex, pons, and certain hypothalamic nuclei. Forebrain cortical regions that receive afferents from the olfactory bulb, such as the anterior olfactory nucleus, olfactory tubercle, prepiriform cortex, entorhinal cortex, and amygdala, exhibited distinct immunoreactivity, while olfactory bulb was almost devoid of staining. Immunoreactivity in the axonal pathways was also found in the limbic–hypothalamic pathways, strionigral projection, and part of the corpus callosum. Results of Western blot analysis and ^3H-$InsP_3$ binding assay were consistent with the qualitative regional differences of immunoreactivity demonstrated by immunohistochemical study. The location of $InsP_3$ receptor in the brain correlates well with the $InsP_3$ binding sites demonstrated by an autoradiographic study.

Many receptors for neurotransmitters in the nervous system are coupled to the phosphoinositide cycle. In that cycle, phosphatidyl inositol bisphosphate is hydrolyzed in response to receptor stimulation to produce inositol 1, 4, 5-trisphosphate ($InsP_3$) and diacylglycerol. $InsP_3$ functions as a second messenger to release calcium from the calcium storage site, the endoplasmic reticulum. By mobilizing intracellular calcium, $InsP_3$ plays diverse roles in many physiological processes (Berridge, 1987; Berridge and Irvine, 1989).

We recently succeeded in cloning and sequencing the cDNA of $InsP_3$ receptor (Furuichi et al., 1989a) and expressing increased $InsP_3$ binding after transfecting NG108 cells with cDNA (Furuichi et al., 1989b). It has been shown that $InsP_3$ receptor, forming a homotetramer, exhibits Ca^{2+} channel activity through binding to the $InsP_3$ molecule (Ferris et al., 1989; Maeda et al., 1991; Miyawaki et al., 1990). $InsP_3$ receptor was found to be identical to a Purkinje cell–enriched glycoprotein called P_{400} (Mallet et al., 1976; Mikoshiba and Changeux, 1978; Mikoshiba et al., 1979, 1985; Maeda et al., 1988, 1989). Therefore, here we will refer to it as the $P_{400}/InsP_3$ receptor. By Western blot analysis, it has been found that P_{400} protein is a ubiquitous protein formed in other parts of the brain (Maeda et al., 1988, 1989). It is of great importance to know what type of cell utilizes the $InsP_3$ receptor system to understand the function and metabolic properties of the cell in the nervous system. In the present study, we determined the distribution of $P_{400}/InsP_3$ receptor by the immunohistochemical method in various areas of adult and developing mouse brain, where we found that the receptor is present in neurons in many areas and that the amount of $P_{400}/InsP_3$ receptor varies from neuron to neuron. We have also performed quantitative analysis by Western blot and by $InsP_3$ binding in some of these areas to substantiate the regional differences observed in the immunohistochemical study.

Materials and Methods

Immunohistochemistry. Pregnant C57BL mice were anesthetized with ether, and the embryos were dissected out. The day of conception was determined by the presence of a vaginal plug [embryonic day 0 (EO)]. E8–E13 embryos were fixed by immersion in fixative overnight at 4°C. Embryos at stages later than E14, pups, and adult mice were fixed by cardiac perfusion. The fixative used was freshly prepared periodate–lysine–paraformaldehyde fixative containing 2% paraformaldehyde, 0.025 mol of L-lysine, and 0.01 mol of periodate in phosphate buffer (pH, 6.2; McLean and Nakane, 1974). Brains were dissected, postfixed in the same fixative overnight at 4°C, and infiltrated with 20% sucrose in 0.1 mol of phosphate buffer (pH, 7.4). Six-micron-thick sections were cut on a cryostat (Miles). The sections were mounted on gelatin-coated slides and stored at −20°C. After being incubated with rabbit normal serum (1:30 dilution; Vector) in Tris-buffered saline (TBS) for 30 min, the sections were incubated with monoclonal antibodies against $P_{400}/InsP_3$ receptor protein for 2 hr. The monoclonal antibodies were prepared as described in a previous paper (Maeda et al., 1988). Sections were incubated in culture medium containing 1 μg of rat immunoglob-

Received July 2, 1990; revised Feb. 5, 1991; accepted Feb. 8, 1991.

We are very grateful to Dr. Allan J. Tobin for critical reading of the manuscript and helpful comments.

Correspondence should be addressed to Dr. S. Nakanishi, Division of Macromolecular Function, Institute for Protein Research, Osaka University, 3-2, Yamadaoka, Suita 565, Japan.

[a] Present address: Institute for Developmental Research, Aichi Prefectural Colony, Kamiyacho, Kasugai, Aichi 480-03, Japan.

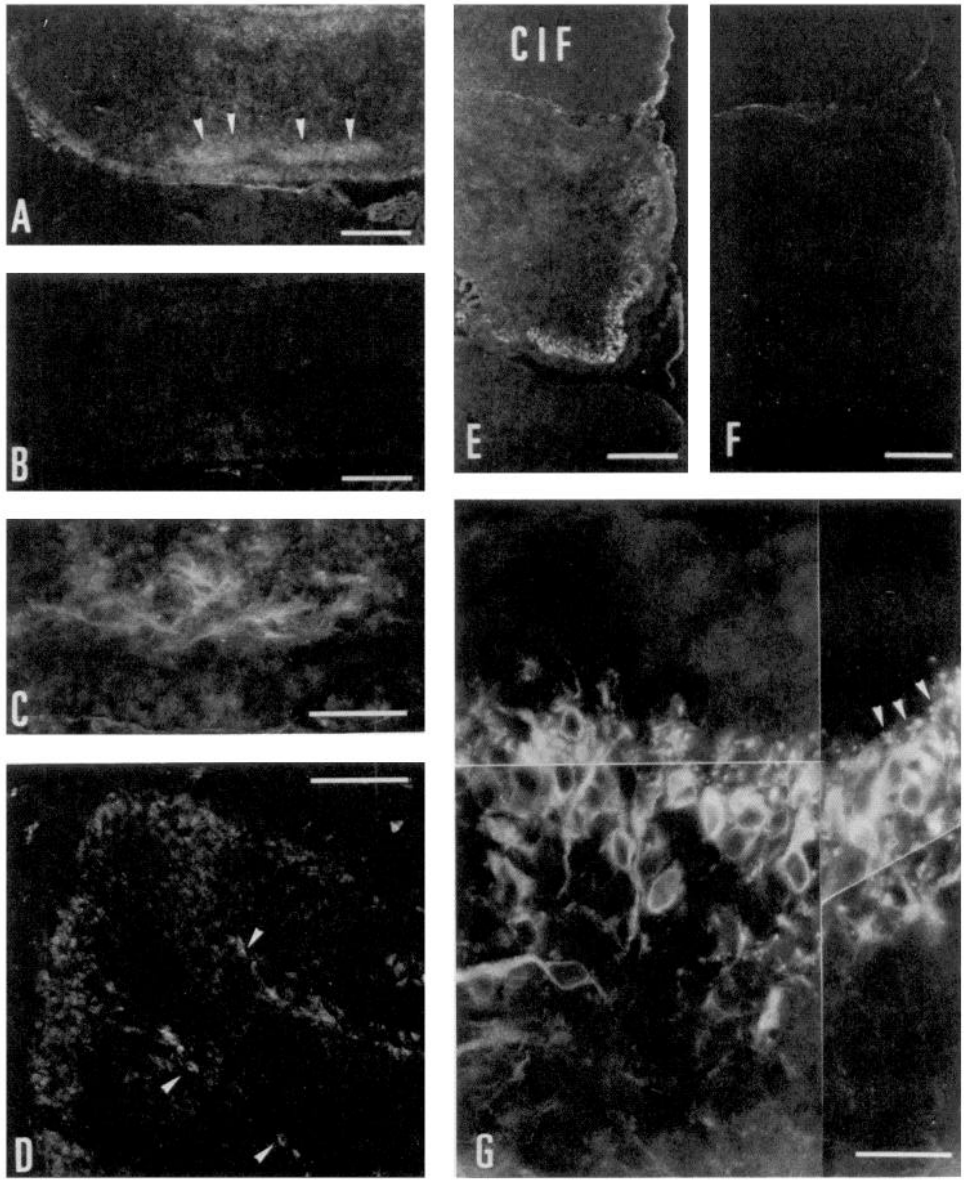

Figure 1. Immunofluorescent localization of $P_{400}/InsP_3$ receptors in developing mouse cerebellum. *A,* At E17, staining with 18A10 occurred in putative Purkinje cells (*arrowheads*) situated in the ventrolateral region of the posterior vermis. Scale bar, 100 μm. *B,* Normal control serum staining of an adjacent section. Scale bar, 100 μm. *C,* Higher magnification of the immunoreactive cells seen in *A*. Perikarya and some processes stained. Scale bar, 25 μm. *D,* At E18, immunoreactive cells (indicated by *arrowheads*) appeared in the rostral region of a coronal section stained with 18A10. Scale bar, 50 μm. *E,* In newborn cerebellum, the distribution of immunoreactive cells extended from the caudal to the rostral region seen in a sagittal section stained with 4C11. *CIF,* inferior colliculus. Scale bar, 100 μm. *F,* Normal control serum staining of an adjacent section. Scale bar, 100 μm. *G,* Higher magnification of the Purkinje cell layer seen in *E*. Perikaryon, apical dendritic process, and axons are stained. Many immunopositive punctate structures (*arrowheads*) seem to represent dendrites. Scale bar, 5 μm.

ulin (Sigma) per milliliter as controls. After two washes with TBS, they were incubated with biotinylated rabbit anti-rat immunoglobulin antiserum (Vector; 1:200 dilution) for 1 hr, then rinsed twice with TBS and incubated with fluorescein isothiocyanate–conjugated avidin in 0.15 mol of HEPES buffer (Vector; 1:200 dilution) for 30 min. All the incubations were at room temperature. The sections were then rinsed with TBS and mounted in buffered glycerol containing 0.1% paraphenylene diamine (Johnson and Nogueira Araujo, 1981). The preparations were examined with a Nikon Optiphot microscope equipped with epi-illumination optics and appropriate filters. Photomicrographs were taken on Kodak TriX-400 film. A confocal microscope (Bio-Rad, MRC-500) equipped with epi-illumination optics was also used. Confocal images were printed out by a color videocopy processor (Mitsubishi, Japan).

Membrane preparation. Tissues were homogenized in 10 vol of 5 mM Tris-HCl (pH, 7.4) containing 0.32 mol of sucrose, 1 mmol of EDTA, 0.1 mmol of phenylmethylsulfonyl fluoride, 10 μmol of pepstatin A, 10 μmol of leupeptin, and 1 mmol of 2-mercaptoethanol. The homogenates were centrifuged at 400,000 × *g* for 30 min at 2°C. The resultant pellets were resuspended in 50 mmol of Tris-HCl (pH, 7.4) containing 1 mmol of EDTA, 0.1 mmol of phenylmethylsulfonyl fluoride, 10 μmol of pepstatin A, 10 μmol of leupepstatin, and 1 mmol of 2-mercaptoethanol. These membrane suspensions were subjected to Western blot or ^3H-$InsP_3$ binding assay as described elsewhere (Maeda et al., 1989, 1990).

Results

Developmental expression of $P_{400}/InsP_3$ receptors in the cerebellum

The location of $P_{400}/InsP_3$ receptors in mouse brain was determined from E8 to the adult stage. Three monoclonal antibodies, 10A6, 4C11, and 18A10 (Maeda et al., 1988, 1989), were compared. Although the intensity of staining differed among them, all of them seemed to recognize the same site on the optical microscope level. Most of the results presented here were obtained on the basis of staining with 18A10 and 4C11. The most conspicuous cellular distribution in developing brain was observed in the Purkinje cells. Because expression on other types of cells was much more discreet than on Purkinje cells, these developmental changes were followed with difficulty.

Immunohistochemical reactions with $P_{400}/InsP_3$ receptors were first detected in some cells in the ventrolateral region of the posterior vermis at E17 (Fig. 1*A–C*). The positions and shapes of these cells were consistent with their being immature Purkinje

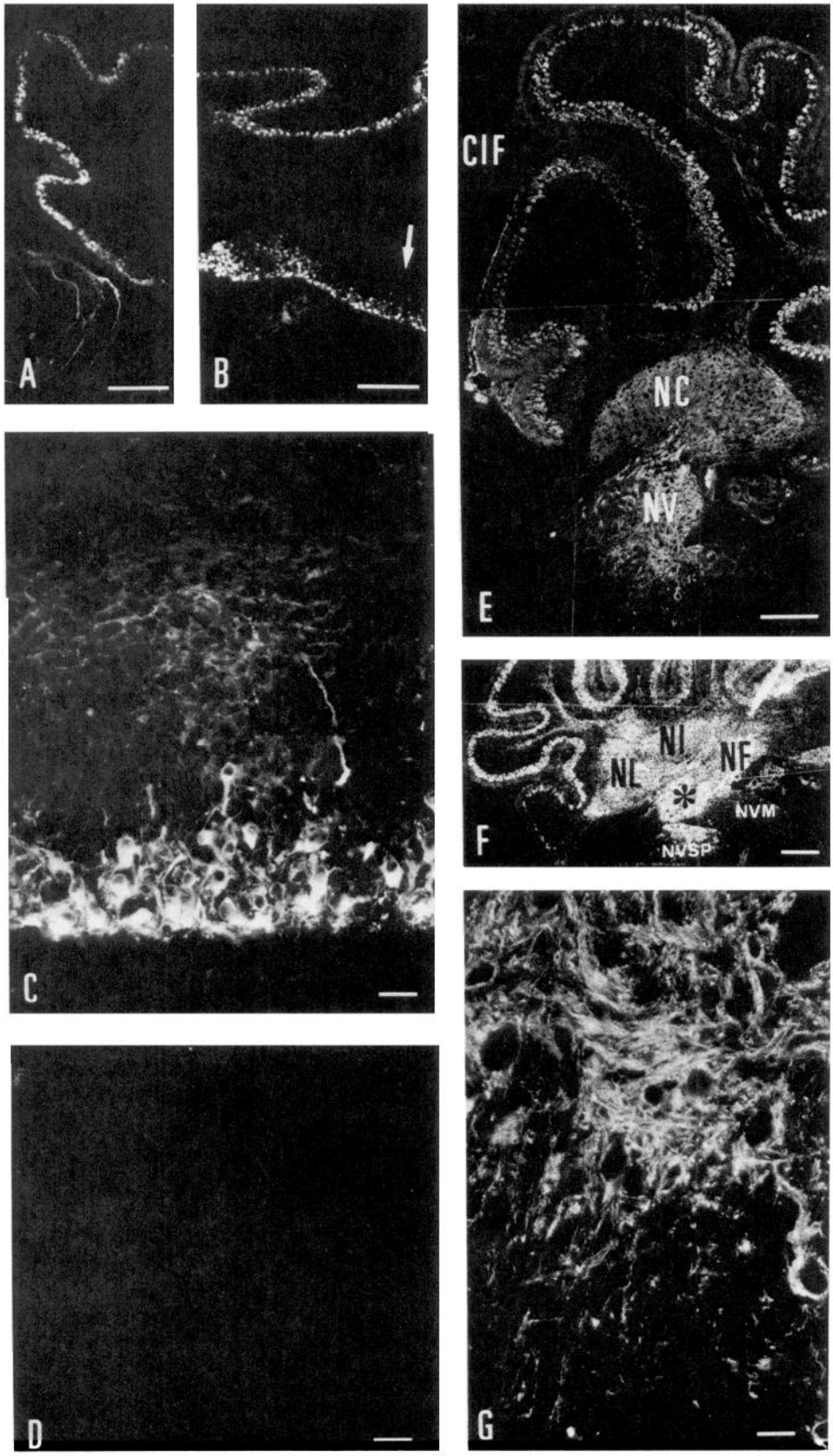

Figure 2. Immunofluorescent localization of $P_{400}/InsP_3$ receptors in developing mouse cerebellum. *A,* At P3, almost the entire Purkinje cell layer stained with 18A10 in the caudal region of a frontal section. Scale bar, 100 μm. *B,* The central region of the same section as *A*. Scale bar, 100 μm. *C,* Higher magnification of a part of the vermis indicated with the *arrow* in *B*. The stained axons of Purkinje cells in the vermis passed through the interstitial space and have come to rest on the surface of the medial cerebellar nuclei. Scale bar, 25 μm. *D,* Normal control serum staining of an adjacent section. Scale bar, 25 μm. *E,* A sagittal section of cerebellum at P7 showed staining of cerebellar nuclei (*NC*) and vestibular (*NV*) nuclei with 4C11. Arborization of Purkinje cell dendrites is present in the molecular layer to some extent. *CIF,* inferior colliculus. Scale bar, 100 μm. *F,* Confocal micrograph of a frontal section passing through the inferior cerebellar peduncle. Intense staining with 4C11 was seen in the axons of Purkinje cells that passed through the white matter, the lateral nucleus (*NL*), the intermediate nucleus (*NI*), and the medial nucleus (*NF*), penetrating the inferior peduncle and terminating on the vestibular nuclei. Among these structures, the most intensely stained was the lateral vestibular nucleus (*asterisk*). The spinal vestibular nucleus (*NVSP*) also stained, but the medial vestibular nucleus (*NVM*) did not. Scale bar, 250 μm. *G,* Higher magnification of a region in the vestibular nuclei of *E*. The cells in the vestibular nuclei failed to stain but are surrounded by intensely immunoreactive fibers. Scale bar, 25 μm.

cells. Perikarya and some dendritic processes stained. At E18 the number of cells and the intensity of staining had increased in the caudolateral region of the cerebellum. Staining was also found in the rostral region in a few cells that seemed to be migrating from the parenchyma towards the future Purkinje cell layer (Fig. 1*D*). In the newborn cerebellum, the distribution of immunoreactive cells in a sagittal section extended from the caudal to the rostral region (Fig. 1*E,F*). At this stage, the Pur-

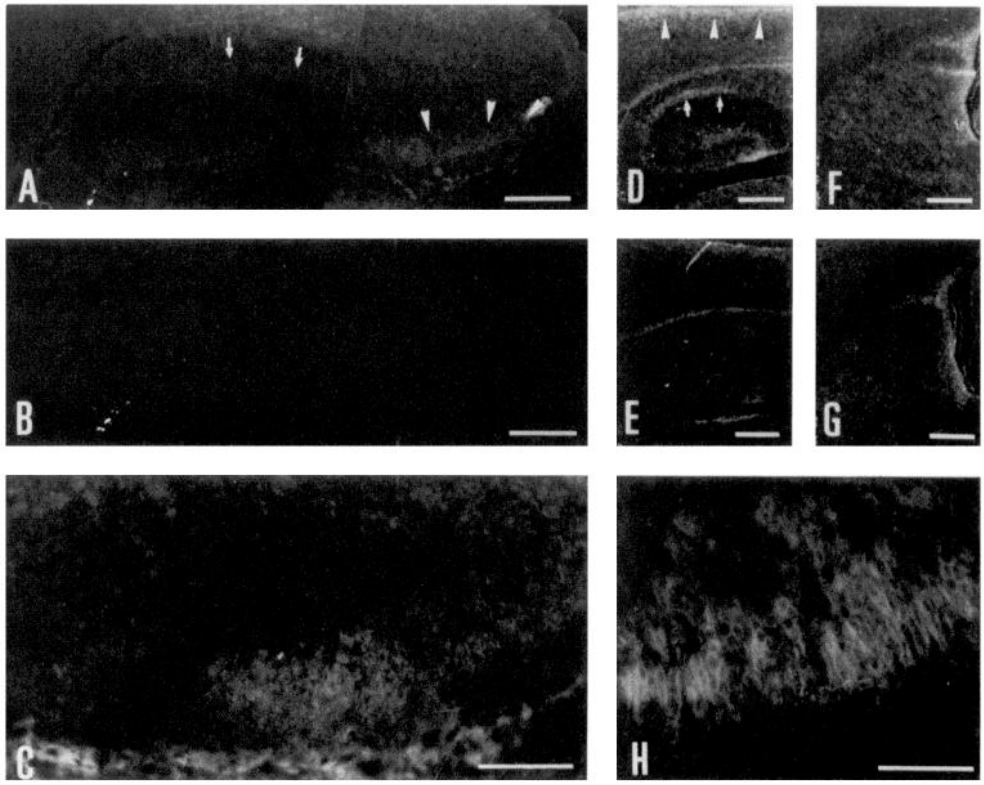

Figure 3. Immunofluorescent localization of $P_{400}/InsP_3$ receptors in structures other than cerebellum in perinatal mouse brain stained with 18A10. *A,* Discrete staining appeared in the retrosplenial cortex of the newborn mouse (*arrowheads*). The hippocampus has not yet stained (*arrows*). Sagittal section. Scale bar, 100 μm. *B,* Normal control serum staining of an adjacent section. Scale bar, 100 μm. *C,* Higher magnification of the region indicated by *arrowheads* in *A*. Scale bar, 25 μm. *D,* Confocal microscopy of immunofluorescent staining in the cerebral cortex (*arrowheads*) and hippocampus (*arrows*) in a sagittal section at P3. *E,* Confocal micrograph of normal control serum staining in an adjacent section. Scale bar, 250 μm. *F,* The striatum in the same section as *D*. It is still devoid of staining. Scale bar, 250 μm. *G,* Normal control serum staining in an adjacent section. Scale bar, 250 μm. *H,* Staining in the retrosplenial cortex at P3. Scale bar, 25 μm.

kinje cell layer consisted of several rows of cells whose orientations were not only vertical, but also horizontal (Fig. 1*G*). Perikarya, apical dendritic processes, and axons stained, while nuclei failed to stain. The apical pole of the somatic cytoplasm stained intensely. Many immunopositive punctate structures situated in the outer part of the perikaryon (Fig. 1*G*, arrowheads) seemed to represent dendrites that were still short, irregular, and divergent, as noted by Ramon y Cajal (1972).

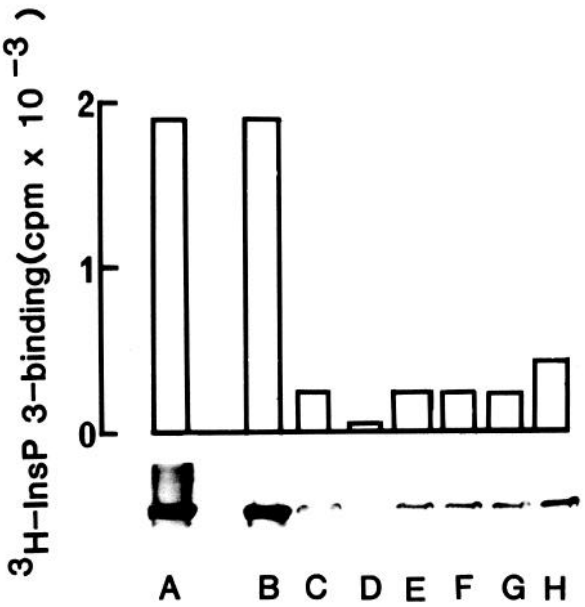

Figure 4. ^{3}H-$InsP_3$ binding assay and Western blot analysis revealed a quantitative regional difference in $P_{400}/InsP_3$ receptor in various areas of the adult mouse brain. *A,* Cerebellum; *B,* cerebellar nuclei; *C,* anterior olfactory nucleus; *D,* substantia nigra; *E,* cerebral cortex; *F,* CA1 region of hippocampus; *G,* hippocampus; *H,* striatum.

At postnatal day 3 (P3), almost the entire Purkinje cell layer from the caudal to the rostral region appeared to stain (Fig. 2*A,B*). In the caudal region, the vermis had an abundance of stained Purkinje cells (Fig. 2*B*). The orientation of most of these cells was vertical. The apical part of the soma was strongly stained, as observed in newborn cerebellum, but dendrites had not yet extended. The axons of these cells seemed to make contact with cells of the cerebellar nuclei, probably of the medial nucleus, whose cells did not stain (Fig. 2*C,D*). The immunoreactive axons of Purkinje cells passed through the interstitial space and came to rest on the surface of these cells. Such localization resulted in the meshwork. By P7, the dendritic arborization of Purkinje cells was apparent. We could also follow clearly stained axons from the white matter down to the deep nuclei (Fig. 2*E,* NC) as well as the vestibular nuclei (Fig. 2*E,* NV). Among the vestibular nuclei, the medial vestibular nucleus was devoid of staining (Fig. 2*F,* NVM). The lateral vestibular nucleus (Fig. 2*F,* asterisk) and the spinal vestibular nucleus (Fig. 2*F,* NVSP) were intensely labeled. Afferent fibers were immunoreactive, while the somata of these nuclei did not stain (Fig. 2*G*). In adult cerebellum, the staining of Purkinje cell axons in the deep nuclei remained distinct as in earlier stages [see Fig. 5*E,* NF (fastigial nucleus or medial deep nucleus of the cerebellum)].

Developmental expression of the $P_{400}/InsP_3$ receptor in other regions of the brain

The $P_{400}/InsP_3$ receptor content in other regions of the brain was much less than in the cerebellum. We nevertheless were able to observe a certain degree of immunoreactivity in the early stages of postnatal development. In the newborn mouse, discreet stain-

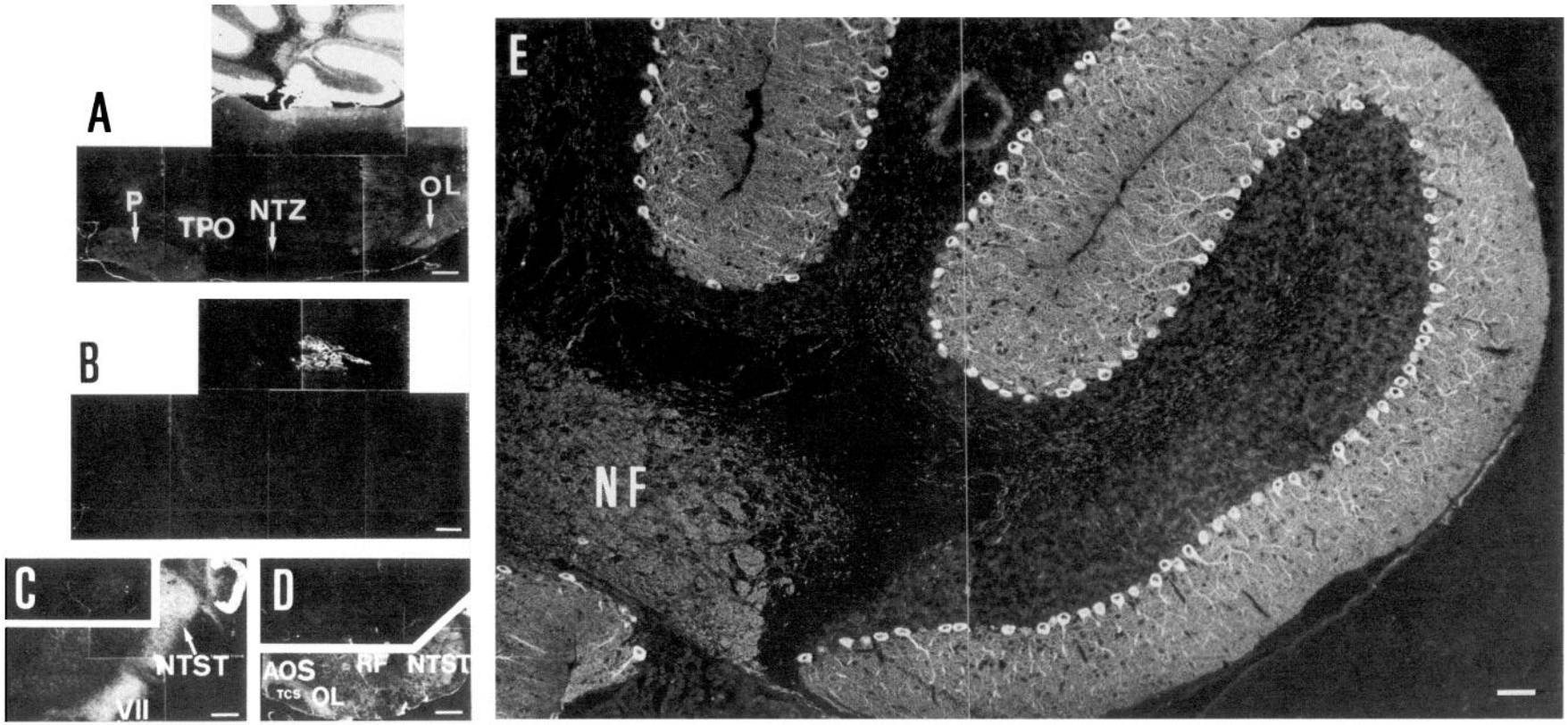

Figure 5. Immunofluorescent localization of $P_{400}/InsP_3$ receptors in adult cerebellum, pons, and medulla oblongata stained with 4C11. *A,* Confocal micrograph of staining in a sagittal section of hindbrain. The most intense immunoreactivity was observed in the Purkinje cell. Fibrous immunoreactivity was seen in the pontine nuclei (*P*), the tegmental nucleus of the pons (*TPO*), the nucleus of the trapezoid body (*NTZ*), the inferior olivary nuclei (*OL*), and the longitudinal fiber tract. Scale bar, 250 μm. *B,* Normal control serum staining of an adjacent section. Scale bar, 250 μm. *C,* Fibrous staining in a frontal section of the medulla oblongata. The nucleus of the facial nerve (*VII*) and the nucleus of the spinal tract of the trigeminal nerve (*NTST*) stained. The *upper left inset* is staining of a control. Scale bar, 250 μm. *D,* Staining in a frontal section of the medulla oblongata at a more caudal level than *A.* In addition to the nucleus of the spinal tract of the trigeminal nerve (*NTST*), the inferior olivary nuclei (*OL*) and the accessory superior olivary nucleus (*AOS*) showed fibrous staining. The reticular formation (*RF*) also stained. The corticospinal tract (*TCS*) was devoid of staining. The *upper panel* is staining of a control. Scale bar, 250 μm. *E,* Higher magnification of the cerebellum. *NF,* fastigial nucleus or medial cerebellar nucleus. Scale bar, 25 μm.

Table 1. Comparisons of immunohistochemical, immunoblotting, and $InsP_3$ binding data

Region	Immunohisto-chemistry	Immuno-blotting	$InsP_3$ binding (cpm)
Telencephalon			
Olfactory bulb	−		
Cerebral cortex	+++	++	231
Hippocampus	+++	++	207
Dentate gyrus	+		
Corpus callosum	+		
Cingulum	−		
Olfactory tubercle	+		
Anterior olfactory nucleus	++	+	238
Nucleus accumbens septi	+++	+++	429
Caudate–putamen	+++	+++	429
Amygdaloid cortex	++		
Prepiriform cortex	++		
Olfactory tract	−		
Anterior commissure	−		
Internal capsule	−		
Precommissural hippocampus	+		
Diencephalon			
Thalamus	−		
Hypothalamus			
Supraoptic nucleus	+		
Mamillary nucleus	+		
Mesencephalon			
Substantia nigra	+	+	31
Pons	+		
Cerebellum			
Whole		++++++	1905
Purkinje-cell layer	++++++++++		
Granular layer	−		
White matter	++		
Cerebellar nuclei	++++	++++	

The relative intensity of immunoreactivity was evaluated using numbers of pluses.

ing occurred in the retrosplenial cortex (Fig. 3*A–C*). At P3, staining in this region was slightly increased. The cells in layer II and III exhibited immunoreactivity in their somata and processes (Fig. 3*H*). The cells of the same layer in the occipital cortex also stained, and the pyramidal cells in the CA1 region of the hippocampus became immunoreactive at this stage, as well (Fig. 3*D,E*). At P7, location of $P_{400}/InsP_3$ receptor in the regions noted above became clearer than in the preceding stage. The immunoreactive cells in the cerebral cortex were located in deeper layers than in the preceding stage. At P15, staining also appeared in the anterior olfactory nucleus (not shown). The striatum, which exhibits abundant immunoreactivity in the adult brain, showed no obvious staining at P3 (Fig. 3*F,G*) and at P15 (not shown).

Expression of $P_{400}/InsP_3$ receptors in adult brain

Although immunoreactivity was most intense in the Purkinje cells in the cerebellum, we also found discrete staining in other areas of the adult brain. These were the striatum, globus pallidus, nucleus accumbens septi, anterior olfactory nucleus, olfactory tubercle, hippocampus, substantia nigra, internal capsule, mamillary nucleus, preoptic nucleus, pons, and cerebral cortex. The intensity of staining differed from area to area. The thalamus showed low immunoreactivity. Structures that showed hardly any immunoreactivity were the olfactory bulb, the anterior commissure, the lateral olfactory tract, and the optic tract. Western blot analysis and ^3H-$InsP_3$ binding assay demonstrated a quantitative regional difference that corresponds well with the intensity of immunohistochemical staining (Fig. 4). Comparisons of immunohistochemical, immunoblotting, and ^3H-$InsP_3$ binding data are shown in Table 1.

Cerebellum, pons, and medulla oblongata

In the adult brain, also, it was the Purkinje cell that expressed the most intense immunoreactivity. The staining of Purkinje cell axons in the deep nuclei remained distinct as in earlier stages (Fig. 5*A,E*). In the pons and medulla oblongata, the staining was restricted to the fibers that pass through the pontine nuclei (Fig. 5*A*, P), the reticular formation (Fig. 5*D*, RF), the nucleus of the trapezoid body (Fig. 5*A*, NTZ), the tegmental nucleus of the pons (Fig. 5*A*, TPO), the inferior olivary nuclei and the accessory superior olivary nucleus (Fig. 5*D*, OL and AOS, respectively), the nucleus of the facial nerve (Fig. 5*C*, VII), and the nucleus of the spinal tract of the trigeminal nerve (Fig. 5*C,D*, NTST). The corticospinal tract was devoid of apparent staining (Fig. 5*D*, TCS).

Cerebral cortex

Areas in the cingulate, retrosplenial, frontal, parietal, occipital, temporal, entorhinal, prepiriform, and amygdaloid cortices were immunoreactive (Fig. 6*A,F,G,J*; 7*A*). In the cingulate and retrosplenial cortex, the staining in layers II–IV was more pronounced than in other cortical layers, probably owing to the cellular density (Fig. 6*F,G*). The cells responsible for such immunoreactivity seem to be the pyramidal cells. Their perinuclear cytoplasm, apical dendrites, and axons stained (Fig. 6*J*). The nucleus was devoid of staining. It was not easy to pursue to what extent the axons of these cells were immunoreactive in the cortical area, but its immunoreactivity was observed in at least part of the corpus callosum (Fig. 6*A*, arrow) and the internal capsule (Fig. 7*D–F*). The internal capsule, which runs through the striatum, did not stain (Fig. 7*C*), but in its posterior part, an irregular, ladderlike structure stained positively (Fig. 7*D–F*).

Hippocampus

The general intensity of staining in the hippocampus was almost the same as that in the cerebral cortex (Fig. 6*A*). This was confirmed by ^{3}H-InsP_3 binding and Western blot analysis (Fig. 4). Although these biochemical analyses did not reveal a significant difference between CA1 and the whole hippocampus, our immunohistochemical results showed that the CA1 region was the most intensely immunoreactive site. The cell that was responsible for the staining in the CA1 region was the pyramidal cell, whose perinuclear cytoplasm and apical dendrites stained in the stratum radiatum and the stratum lacunosum (moleculare), where they ramify and make contact with afferent fibers (Fig. 6*D,E*). The dentate gyrus also stained, but to a lesser extent. The staining in the CA2 and CA3 regions was less intense than in the CA1 region.

Striatum and substantia nigra

Next to the cerebellar nuclei, the striatum exhibited the most intense immunoreactivity. Western blot and ^{3}H-InsP_3 binding assays confirmed the relatively high level of InsP_3 receptor (Fig. 4). The most strongly labeled cells in the striatum (Fig. 7*C*) were as large as the pyramidal cells in the cerebral cortex (Fig. 6*J*). Some smaller cells also stained, as did a surrounding fiber meshwork (Fig. 7*C*). The internal capsule fibers, which run through this structure, did not stain significantly. The globus pallidus, which lies next to the caudate and receives strong afferents from the caudate and putamen, also stained (not shown). The substantia nigra, on which a part of the efferent pathways from the caudate and putamen project, stained weakly (Fig. 7*G–I*). In this structure, the reticular fibers stained (Fig. 7*H*).

Structures related to the limbic system and other structures

The immunoreactivity in the hippocampus was described above.

The olfactory bulb did not stain. Neither the somata of the olfactory bulb nor the olfactory tract demonstrated any immunoreactivity. In contrast, the structures to which the olfactory tract sends fibers showed conspicuous immunoreactivity. These were the anterior olfactory nucleus (Fig. 6*C*, OA), the olfactory tubercle (Fig. 7*A*, TUO), the nucleus accumbens septi (Fig. 6*C*, ACB), the amygdaloid cortex (Fig. 7*D,E*), and the precommissural hippocampus (Fig. 6*F–H*). The prepiriform cortex, which is continuous with the anterior olfactory nucleus, also stained (Fig. 7*A*).

In all these structures, both the somata and some fiber processes stained. In contrast with these findings, the staining in the following structures was largely restricted to the fibers: the hypothalamic nuclei such as the mamillary nucleus, the preoptic nucleus, the lateral hypothalamic nucleus, and certain fasciculi that run through these areas (not shown).

Discussion

In the present study, we used immunohistochemistry to determine the distribution of P_{400}/InsP_3 receptors in the adult and developing mouse brain. In the developing cerebellum, Purkinje cells expressed a P_{400}/InsP_3 receptor as early as E17–E18. Maeda et al. (1989) detected P_{400} protein in mouse cerebellum immunohistochemically from P3 on but not before. This discrepancy seems to be due to a methodological difference. The fixative and the immunohistochemical procedure we used in this study enabled us to visualize immunoreactive neurons in detail. From the perinatal through the postnatal period of development, the

→

Figure 6. Immunofluorescent localization of P_{400}/InsP_3 receptors in adult mouse brain. *A*, Confocal micrograph of a sagittal section showing staining with 18A10 in the hippocampus and the cerebral cortex. Pyramidal cells in the CA1 region of the hippocampus showed relatively intense staining. The dentate gyrus stained to a lesser extent. Part of the corpus callosum stained weakly (*arrow*). The lateral thalamic nucleus (*asterisk*) did not stain. Scale bar, 250 μm. *B*, Confocal micrograph of normal control serum staining in an adjacent section. Scale bar, 250 μm. *C*, Confocal micrograph of a sagittal section showed staining with 18A10 in the anterior olfactory nucleus (*OA*), the nucleus accumbens septi (*ACB*; lateral parolfactorial area), and the striatum (*CPU*). The olfactory tract (*TO*), the anterior commissure (*CA*), and the internal capsule in the striatum (*arrow*) did not stain. Scale bar, 250 μm. *D*, Higher magnification of CA1 region. Perinuclear cytoplasm and apical dendrites stained in the stratum radiatum and stratum lacunosum (moleculare). Scale bar, 25 μm. *E*, Normal control serum staining in an adjacent section. Scale bar, 25 μm. *F*, A frontal section, showing immunoreactive cells in the cingulate cortex and in the precommissural hippocampus (*PH*) stained with 4C11. Scale bar, 100 μm. *G*, Normal control serum staining in an adjacent section. Scale bar, 100 μm. *H*, Higher magnification of a region in the precommisural hippocampus. Some cells were immunoreactive. Scale bar, 25 μm. *I*, Higher magnification of a region of the anterior olfactory nucleus (*right half*) and the nucleus accumbens septi (*left half*) stained with 18A10. Perinuclear cytoplasm was immunoreactive. Scale bar, 25 μm. *J*, Higher magnification of a region in the cingulate cortex. Perinuclear cytoplasm, axon, and apical dendrites stained. Scale bar, 25 μm.

Figure 7. Immunofluorescent localization of P_{400}/InsP_3 receptors in adult mouse brain. *A*, A confocal micrograph of a frontal section. The striatum (*CPU*), the prepiriform cortex (*PIR*), and the olfactory tubercle (*TUO*) were stained with 18A10. The lateral olfactory tract (*TOL*) and the anterior commissure (*CA*) were devoid of staining. The *inset* shows control staining. Scale bar, 250 μm. *B*, Normal control serum staining in a section adjacent to *C*. Scale bar, 25 μm. *C*, Higher magnification of part of the striatum seen in a conventional microscope showed intense staining in the perinuclear cytoplasm. A fiber meshwork surrounds these positively stained cells. The internal capsule did not stain. Scale bar, 25 μm. *D*, Confocal micrograph of a frontal section, showing staining with 18A10 in the internal capsule (*CI*). The optic tract (*OT*) was devoid of staining. The medial amygdaloid nucleus (*AME*) stained. Scale bar, 250 μm. *E*, Control staining in an adjacent section. Scale bar, 250 μm. *F*, Higher magnification of the internal capsule. An irregular, fibrous, ladderlike structure stained. Scale bar, 25 μm. *G*, Frontal section, showing staining with 4C11 in the substantia nigra (*SN*). *DG*, dentate gyrus; *CGL*, lateral geniculate body. Scale bar, 100 μm. *H*, Higher magnification of the substantia nigra seen in *G*. No obvious somatic staining was observed but the reticular fibers stained. Scale bar, 25 μm. *I*, Normal control serum staining of a section adjacent to *G.CA3*, CA3 region of the hippocampus.

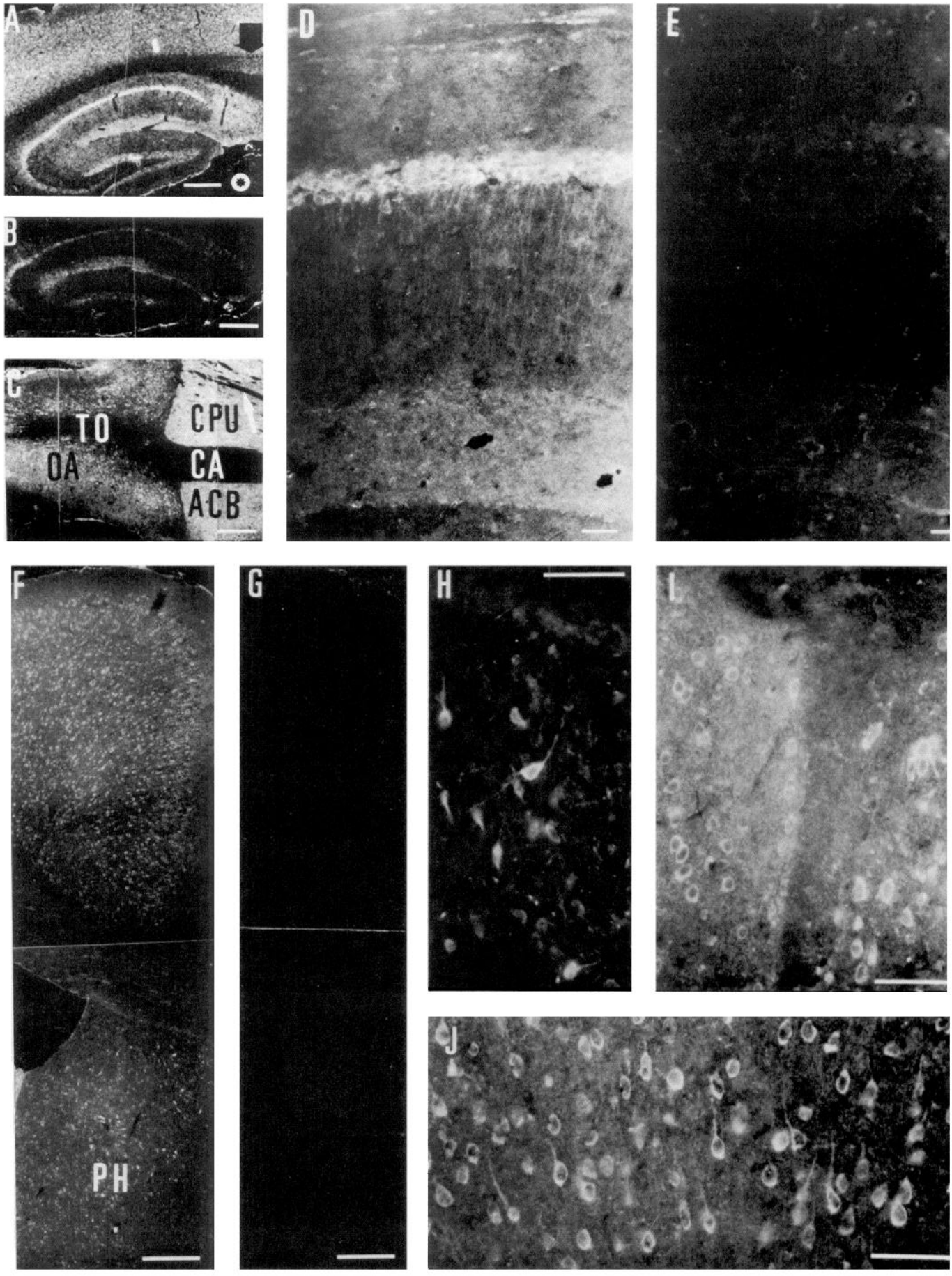
A
B
C
TO
OA
CPU
CA
ACB
D
E
F
PH
G
H
I
J

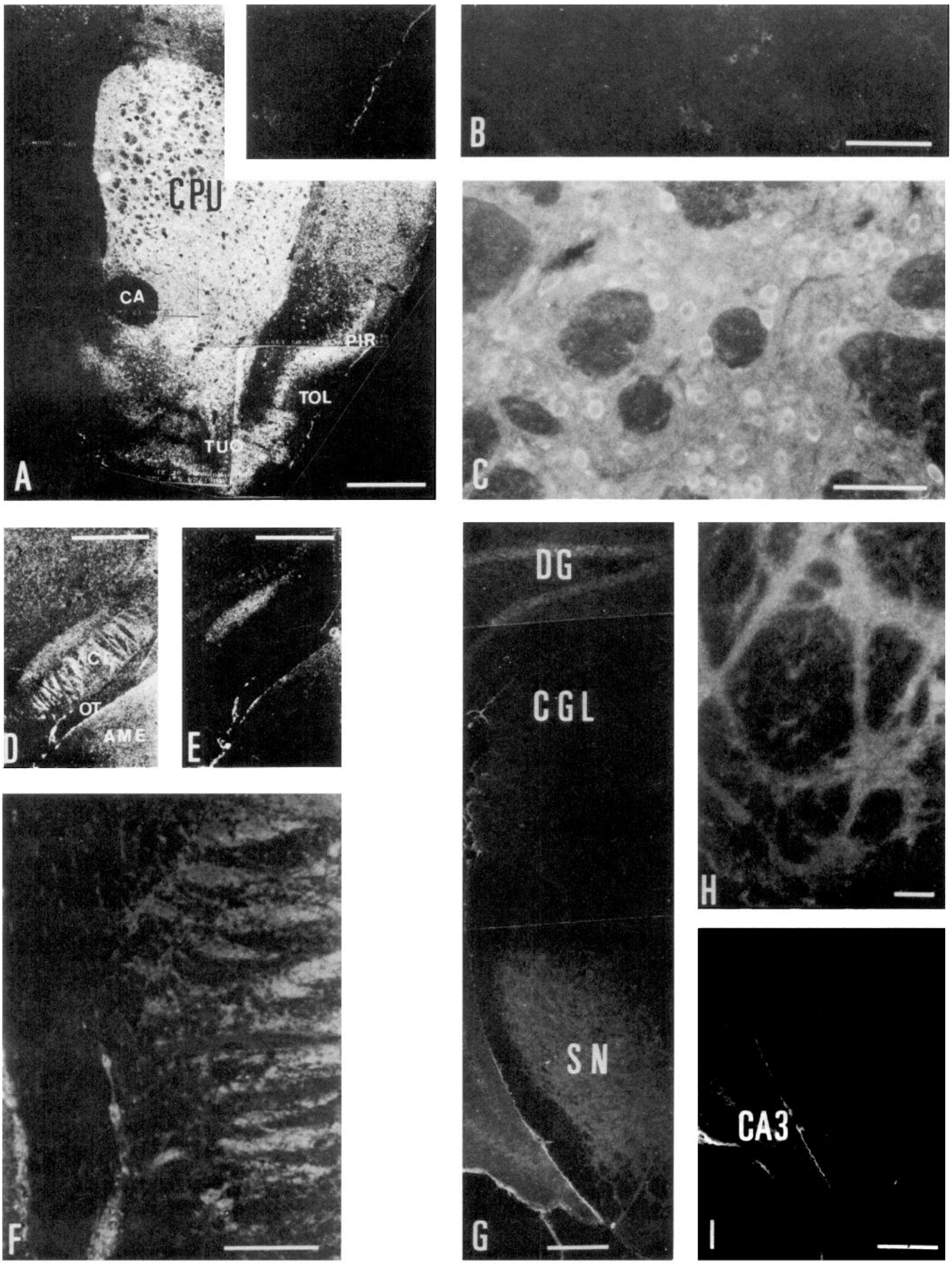
CPU
CA
PIR
TOL
TUO
A
B
C
D
OT
AME
E
DG
CGL
SN
G
H
CA3
I
F

expression of a $P_{400}/InsP_3$ receptor in Purkinje cells appears to follow the general lateromedial and caudorostral developmental gradient. In the mouse embryo, Purkinje cells originate on E11–E14 and remain quiescent for several days after their generation and migration. Although it is believed that evident growth of the Purkinje cell soma does not begin until after birth (Altman, 1982), the present results demonstrate that the so-called immature perinatal Purkinje cell already expresses an $InsP_3$ receptor, and this may be its earliest expression, at least in the CNS.

Localization detected at the level of the cerebellar nuclei as well as the vestibular nuclei represents the location of $P_{400}/InsP_3$ receptors at the presynaptic terminal of the Purkinje cell's axonal projections to these structures. Although the afferents from the vestibule terminate in all of the vestibular nuclei, the medial vestibular nucleus was devoid of staining. In an autoradiographic study in developing rat brain, $InsP_3$ binding was first detected in the newborn rat cerebellum (Worley et al., 1989). At P5, $InsP_3$ binding became pronounced in both the molecular layer of the cerebellar cortex and the cerebellar nuclei. The present findings correspond well with these observations.

Purkinje cells are physiologically excitable, and their axons reach the white matter 1 d after birth in the rat (Shimono et al., 1976). At this stage, their electroresponsive properties are basically dominated by sodium currents. At the third or fourth day, some Purkinje cells show calcium responses (Llinas and Sugimori, 1979). Expression of electrophysiological properties in the cultured immature Purkinje cell is also reported (Gruol and Franklin, 1987). The existence of the $InsP_3$ receptor in Purkinje cell axons and at axon terminals at P3 is consistent with the development of such function.

Phosphatidyl inositol turnover is highly coupled to a quisqualate-type glutamate receptor in the cerebellum (Bredt and Snyder, 1989; Garthwaite et al., 1989), coinciding with the finding that the Purkinje cells in the cerebellum are particularly rich in $InsP_3$ receptors (Worley et al., 1987, 1989; Furuichi et al., 1989b; Maeda et al., 1990) and glutamate receptors (Keinänen et al., 1990). There is classic evidence that the stimulation of Purkinje cells results in hyperpolarization of postsynaptic cells in these structures after releasing GABA as a neurotransmitter. GABA receptors are presently not considered to be coupled to phosphoinositide turnover. This coincides well with the low expression of $InsP_3$ receptors by cells in the cerebellar nuclei as well as the vestibular nuclei.

With regard to the localization of the $P_{400}/InsP_3$ receptor in other areas of the brain at a given stage of development, not all the positively stained sites in adult brain express immunoreactivity. For example, the striatum exhibits relatively intense staining in the adult brain, but not at younger stages. This suggests the possibility that the protein kinase C limb of the pathway plays a more important role than $InsP_3$ receptor at these stages.

In the adult brain, though immunoreactivity was most intense in the Purkinje cell, we also found somatic and/or fibrous staining in other areas. Most of the structures referred to as the olfactory brain expressed a relatively significant amount of this receptor, as did the nonolfactory telencephalon, which represents phylogenetically the newest structures. These were the striatum, globus pallidus, nucleus accumbens septi, anterior olfactory nucleus, olfactory tubercle, hippocampus, substantia nigra, internal capsule, mamillary nucleus, preoptic nucleus, pontine nuclei, facial nerve nuclei, inferior olivary nucleus, and cerebral cortex. The intensity of staining differed from area to area. The most intensely stained regions next to the cerebellum were the striatum and the nucleus accumbens septi, followed by the cerebral cortex, hippocampus, olfactory tubercle, and anterior olfactory nucleus. The other areas were only moderately stained. Such localization of $P_{400}/InsP_3$ receptor largely corresponds to that of the membrane-bound phospholipase C activities (Nishida et al., 1988). Localization of $InsP_3$ binding was demonstrated in the sections of rat brain by an autoradiographic study (Worley et al., 1987, 1989). The autoradiographic data of $InsP_3$ binding roughly correspond to our immunohistochemical results. The quantitative analyses done in the present study also showed a good correlation with immunohistochemical findings.

Among the structures that belong to the primary olfactory system of the olfactory brain, the olfactory bulb, which is massively developed in this macrosomatic animal, was almost devoid of staining, in contrast to the distinct immunoreactivity in the forebrain cortical regions that receive the afferents from the olfactory bulb. This was consistent with an autoradiographic study in which the $InsP_3$ binding sites were not detectable in the olfactory bulb (Worley et al., 1987, 1989). Many neuroactive substances, neurotransmitters as well as neuromodulators, are found in the olfactory bulb, and some of them are reported to be involved in the receptor-activated phosphoinositide turnover in other neuronal systems. Protein kinase C, another important component of the inositol phospholipid pathway, has been shown to be present in the olfactory bulb (Worley et al., 1987, 1989). These results suggest that the protein kinase C limb of the pathway has an important role in this structure.

In addition, the distribution of a calcium-binding protein, calbindin, resembles that of ^3H-$InsP_3$ binding sites. Comparison of immunohistochemical data on calbindin (Jande et al., 1981; Baimbridge and Miller, 1982; Feldman and Christakos, 1983; Garcia-Segura et al., 1984; Gerfen et al., 1985; Kiyama et al., 1985; Yoshida et al., 1985) and the present $P_{400}/InsP_3$ receptor study showed a certain resemblance in their localization, though there exists a discrepancy among the immunohistochemical data on calbindin. According to the immunohistochemical data, calbindin was located in the olfactory bulb (Jande et al., 1981; Baimbridge and Miller, 1982; Garcia-Segura et al., 1984), but $P_{400}/InsP_3$ receptor was not found there as mentioned above. On the other hand, *in situ* hybridization data on calbindin showed a general correspondence of the distribution of calbindin and $InsP_3$ receptor except in the olfactory bulb; no mRNA existed in the olfactory bulb (G. D. Frantz and A. J. Tobin, Department of Biology, UCLA, personal communication). It seems that further analysis may be required to determine the relationship between these proteins.

One of the structures referred to as nonolfactory telencephalon, the striatum, exhibited a relatively high $P_{400}/InsP_3$ receptor content. The striatum possesses complex intrinsic and extrinsic connections and contains a variety of neurotransmitters. Given the complexity of structure and physiological significance, it is not surprising that the striatum contains a large amount of $P_{400}/InsP_3$ receptor coupled to diverse receptors. For example, a glutamatergic receptor that may be coupled to phosphoinositide turnover has been found in a primary culture of striatal neurons (Sladeczek et al., 1985). Relatively large neurons and fiber meshwork were immunoreactive. The nature of these neurons and fibers remains to be determined. In an immunohistochemical study of $InsP_3$ receptor localization in the rat brain, low levels of immunoreactivity were detected in medium spiny neurons, though the data were not shown (Mignery et al., 1989). The positively stained fiber meshwork seems to involve the local

collaterals of these neurons. The thalamocortical projection that runs through the entire striatum may also be involved in the positively stained fiber meshwork, though the immunoreactivity of the thalamus was low. The globus pallidus and the substantia nigra, to which the medium spiny type I neurons in the striatum project, also stained. The fibrous immunoreactivity in the substantia nigra may represent the existence of two projections, strionigral and corticonigral fibers. The strionigral efferent pathway sends its fibers mostly through the internal capsule, bypassing the globus pallidus, and most of them project to the pars reticulata of the substantia nigra. On the other hand, the corticonigral pathway passes through the internal capsule in the striatum, which was devoid of staining. The positively stained posterior part of the internal capsule seemed to represent the fibers from the globus pallidus that terminate in the hypothalamic nucleus. These findings suggest that the immunopositive fibers found in the substantia nigra represent the strionigral projection.

Another nonolfactory telencephalon structure that also expressed a relatively high level of immunoreactivity was the neocortex. The weakly stained corpus callosum indicates the presence of P_{400}/$InsP_3$ receptor in the corticofugal fibers. The caudal part of the internal capsule also showed a certain degree of immunoreactivity. All corticofugal neurons that send fibers to the internal capsule send collaterals to the corpus callosum. This suggests another possibility, in addition to that mentioned above: that they represent the efferents from the cerebral cortex projected to the brain stem and spinal cord, though the exact destinations of these immunopositive fibers remains to be determined.

In summary, a variety of neurons expressed the $InsP_3$ receptor in various areas of the brain. Many of the areas, however, where the $InsP_3$ receptor density is low in adult brain as well as in developing brain are considered to exhibit coupling of various neurotransmitter receptors to phosphoinositide turnover. Therefore, further analysis is required to clarify the relationship between $InsP_3$ receptor and cellular function. The present findings provide much new information for studying the phosphoinositide-associated messengers in the brain that function in many physiological processes such as mediation of the primary signal of neurotransmission, modulation of neuronal signals, and secretion.

References

Altman J (1982) Morphological development of the rat cerebellum and some of its mechanisms. Exp Brain Res [Suppl] 6:8–49.

Baimbridge KG, Miller JJ (1982) Immunohistochemical localization of calcium-binding protein in the cerebellum, hippocampal formation and olfactory bulb of the rat. Brain Res 245:223–229.

Berridge MJ (1987) Inositol trisphosphate and diacylglycerol: two interacting second messengers. Annu Rev Biochem 56:159–193.

Berridge MJ, Irvine RF (1989) Inositol phosphates and cell signalling. Nature 341:197–205.

Bredt DS, Snyder SH (1989) Nitric oxide mediates glutamate-linked enhancement of cGMP levels in the cerebellum. Proc Natl Acad Sci USA 86:9030–9033.

Feldman SC, Christakos S (1983) Vitamin D-dependent calcium-binding protein in rat brain: biochemical and immunocytochemical characterization. Endocrinology 112:290–302.

Ferris CD, Huganir RL, Supattapone S, Snyder SH (1989) Purified inositol 1, 4, 5-trisphosphate receptor mediates calcium flux in reconstituted lipid vesicles. Nature 342:87–89.

Furuichi T, Yoshikawa S, Mikoshiba K (1989a) Nucleotide sequence of cDNA encoding P_{400} protein in the mouse cerebellum. Nucleic Acids Res 17:5385–5386.

Furuichi T, Yoshikawa S, Miyawaki A, Wada K, Maeda N, Mikoshiba K (1989b) Primary structure and functional expression of the inositol 1, 4, 5-trisphosphate–binding protein P_{400}. Nature 342:32–38.

Garcia-Segura LM, Baetens D, Roth J, Norman AW, Orci L (1984) Immunohistochemical mapping of calcium-binding protein immunoreactivity in the rat central nervous system. Brain Res 296:75–86.

Garthwaite J, Southam E, Anderton M (1989) A kainate receptor linked to nitric oxide synthesis from arginine. J Neurochem 53:1952–1954.

Gerfen CR, Baimbridge KG, Miller JJ (1985) The neostriatal mosaic: compartmental distribution of calcium-binding protein and parvalbumin in the basal ganglia of the rat and monkey. Proc Natl Acad Sci USA 82:8780–8784.

Gruol DL, Franklin CL (1987) Morphological and physiological differentiation of Purkinje neurons in cultures of rat cerebellum. J Neurosci 7:1271–1293.

Jande SS, Tolnai S, Lawson DEM (1981) Immunohistochemical localization of vitamin D–dependent calcium-binding protein in duodenum, kidney, uterus and cerebellum of chickens. Histochemistry 71:99–116.

Johnson GD, Nogueira Araujo GM (1981) A simple method of reducing the fading of immunofluorescence during microscopy. J Immunol Methods 43:349–350.

Keinänen K, Wisden W, Sommer B, Werner P, Herb A, Verdoorn TA, Sakmann B, Seeburg PH (1990) A family of AMPA-selective glutamate receptors. Science 249:556–560.

Kiyama H, Takami K, Hatakenaka S, Nomura I, Tohyama M, Miki N (1985) Localization of chick retical 24,000 dalton protein (Visinin)–like immunoreactivity in the rat lower brain stem. Neuroscience 14: 547–556.

Llinas R, Sugimori M (1979) Calcium conductances in Purkinje cell dendrites: their role in development and integration. Prog Brain Res 51:1724–1730.

Maeda N, Niinobe M, Nakahira K, Mikoshiba K (1988) Purification and characterization of P_{400} protein, a glycoprotein characteristic of Purkinje cell, from mouse cerebellum. J Neurochem 51:1724–1730.

Maeda N, Niinobe M, Inoue Y, Mikoshiba K (1989) Developmental expression and intracellular location of P_{400} protein characteristic of Purkinje cells in the mouse cerebellum. Dev Biol 133:67–76.

Maeda N, Niinobe M, Mikoshiba K (1990) A cerebellar Purkinje cell marker P_{400} protein is an inositol 1, 4, 5-trisphosphate ($InsP_3$) receptor protein. EMBO J 9:61–68.

Maeda N, Kawasaki T, Nakade S, Yokota N, Taguchi T, Kasai M, Mikoshiba K (1991) Structural and functional characterization of inositol 1,4,5-trisphosphate receptor channel from mouse cerebellum. J Biol Chem 266:1109–1116.

Mallet J, Huchet M, Pougeois R, Changeux JP (1976) Anatomical, physiological and biochemical studies on the cerebellum from mutant mice. III. Protein differences associated with the *weaver, staggerer* and *nervous* mutations. Brain Res 103:291–312.

McLean IW, Nakane PK (1974) Peroxidase–lysine–paraformaldehyde fixative. A new fixative for immunoelectron microscopy. J Histochem Cytochem 22:1077–1083.

Mignery GA, Sudhof TC, Takei K, De Camilli P (1989) Putative receptor for inositol 1, 4, 5-trisphosphate similar to ryanodine receptor. Nature 342:192–195.

Mikoshiba K, Changeux JP (1978) Morphological and biochemical studies on isolated molecular and granular layers from bovine cerebellum. Brain Res 142:487–504.

Mikoshiba K, Huchet M, Changeux JP (1979) Biochemical and immunological studies on the P_{400} protein, a protein characteristic of the Purkinje cell from mouse and rat cerebellum. Dev Neurosci 2:254–275.

Mikoshiba K, Okano H, Tsukada Y (1985) P_{400} protein characteristic to Purkinje cells and related proteins in cerebella from neuropathological mutant mice: autoradiographic study by ^{14}C-leucine and phosphorylation. Dev Neurosci 7:179–185.

Miyawaki A, Furuichi T, Maeda N, Mikoshiba K (1990) Expressed cerebellar-type inositol 1, 4, 5-trisphosphate receptor, P_{400}, has calcium release activity in a fibroblast L cell line. Neuron 5:11–18.

Nishida A, Kaiya H, Tohmatsu T, Banno Y, Wakabayashi S, Nozawa Y (1988) Regional distribution of phosphoinositide-specific phospholipase C activity in rat brain. Neurosci Lett 90:354–357.

Ramon y Cajal S (1972) Histologie du systeme nerveux de l'homme

et des vertebres, pp 94. Madrid: Consejo Superior de Investigaciones Cientificas Instituto Ramon y Cajal.

Shimono T, Nosaka S, Sasaki S (1976) Electrophysiological study on the postnatal development of neuronal mechanisms in the rat cerebellar cortex. Brain Res 108:279–294.

Sladeczek F, Pin JP, Recasens M, Bockaert J, Weiss S (1985) Glutamate stimulates inositol phosphate formation in striatal neurons. Nature 317:717–719.

Worley PF, Baraban JM, Supattapone S, Wilson VS, Snyder SH (1987) Characterization of inositol trisphosphate receptor binding in brain. J Biol Chem 262:12132–12136.

Worley PF, Baraban JM, Snyder SH (1989) Inositol 1, 4, 5-trisphosphate receptor binding: autoradiographic localization in rat brain. J Neurosci 9:339–346.

Yoshida S, Kiyama H, Tohyama M, Hatakenaka S, Miki N (1985) Ontogeny of Visinin-like immunoreactive structures in the rat cerebellum and vestibular nuclei: an immunohistochemical analysis. Dev Brain Res 22:247–253.